4

Gouy Phase and Matter Waves

Irismar G. da Paz[1], Maria C. Nemes[2] and José G. P. de Faria[3]
[1]*Departamento de Física, Universidade Federal do Piauí e Universidade Federal de Minas Gerais*
[2]*Departamento de Física, Universidade Federal de Minas Gerais*
[3]*Departamento de Física e Matemática, Centro Federal de Educação Tecnológica de Minas Gerais*
Brazil

1. Introduction

Schrödinger conceived his wave equation having in mind de Broglie's famous relation from which we learnt to attribute complementary behavior to quantum objects depending on the experimental situation in question. He also thought of a wave in the sense of classical waves, like electromagnetic waves and others. However, the space-time asymmetry of the equation with governs quantum phenomena lead the scientific community to investigate the new physics this specific wave was about to unveil. It turns out that in certain experimental condition classical light has its behavior dictated by a bidimensional Schrödinger equation for a free particle. This fact is well known for several years (Yariv, 1991; Snyder & Love, 1991; Berman, 1997; Marte & Stenholm, 1997). For this special kind of waves it is possible to define the analog of a Hilbert space and operators which do not commute (as reviewed in section 2) in such a way that the mathematical analogy becomes perfect. A natural question emerging in this context, and the case of the present investigation is the following: how far, in the sense of leaning new physics, can we take this analogy ?

We have been able to show that the generalized uncertainty relation by Robertson and Schrödinger, naturally valid for paraxial waves, can shed new light on the physical context of a beautiful phenomenon, long discovered by Gouy (Gouy, 1890; 1891) which is an anomalous phase that light waves suffer in their passage by spatial confinement. This famous phase is directly related to the covariance between momentum and position and since for the "free particles" we are considering $\sigma_{xx}\sigma_{pp} - \sigma_{xp}^2 = constant$ we see that Gouy phase can be indirectly measured from the coordinate and momentum variances, quantities a lot easier to measure than covariance between x and p. On the other hand, as far as free atomic particles are concerned, experiments elaborated to test the uncertainty relation (Nairz et al., 2002) will reveal to us the matter wave equivalence of Gouy phase. Unfortunately the above quoted experiment was not designed to determine the phase and that is the reason why, so far, we have only an indirect evidence of the compatibility of theory and experiment. The last aim of our research is to try to encourage laboratories with facilities involving microwave cavities and atomic beams to perform an experiment to obtain the Gouy phase for matter waves.

We believe that Gouy phase for matter waves could have important applications in the field of quantum information. The transversal wavefunction of an atom in a beam state can be treated not only as a continuous variable system, but also as an infinite-dimensional discrete system.

The atomic wavefunction can be decomposed in Hermite-Gaussian or Laguerre-Gaussian modes in the same way as an optical beam (Saleh & Teich, 1991), which form an infinite discrete basis. This basis was used, for instance, to demonstrate entanglement in a two-photon system (Mair et al., 2001). However, it is essential for realizing quantum information tasks that we have the ability to transform the states from one mode to another, making rotations in the quantum state. This can be done using the Gouy phase, constructing mode converters in the same way as for light beams (Allen et al., 1992; Beijersbergen et al., 1993). In a recent paper is discussed how to improved electron microscopy of magnetic and biological specimens using a Laguere-Gauss beam of electron waves which contains a Gouy phase term (McMorran et al., 2011).

2. Analogy between paraxial equation and Schrödinger equation

One of the main differences in the dynamical behavior of electromagnetic and matter waves relies in their dispersion relations. Free electromagnetic wave packets in vacuum propagate without distortions while, *e.g.*, an initially narrow gaussian wave function of a free particle tends to increase its width indefinitely. However, the paraxial approximation to the propagation of a light wave in vacuum is formally identical to Schrödinger's equation. In this case they are bound to yield identical results.

We start our analysis by taking the simple route of a direct comparison between the Gaussian solutions of the paraxial wave equation and the two-dimensional Schrödinger equation.

Consider a stationary electric field in vacuum

$$E(\vec{r}) = A(\vec{r}) \exp(ikz). \tag{1}$$

The paraxial approximation consists in assuming that the complex envelope function $A(\vec{r})$ varies slowly with z such that $\partial^2 A/\partial z^2$ may be disregarded when compared to $k\partial A/\partial z$. In this condition, the approximate wave equation can be immediately obtained and reads (Saleh & Teich, 1991)

$$\left(\frac{\partial^2}{\partial x^2} + \frac{\partial^2}{\partial y^2} + i4\pi \frac{1}{\lambda_L} \frac{\partial}{\partial z} \right) A(x, y, z) = 0, \tag{2}$$

where λ_L is the light wavelength.

Consider now the two-dimensional Schrödinger equation for a free particle of mass m

$$\left(\frac{\partial^2}{\partial x^2} + \frac{\partial^2}{\partial y^2} + 2i \frac{m}{\hbar} \frac{\partial}{\partial t} \right) \psi(x, y, t) = 0. \tag{3}$$

Here, $\psi(x, y, t)$ stands for the wave function of the particle in time t. Assuming that the longitudinal momentum component p_z is well-defined (Viale et al., 2003), i.e., $\Delta p_z \ll p_z$, we can consider that the particle's movement in the z direction is classical and its velocity in this direction remains constant. In this case one can interpret the time variation Δt as proportional to Δz, according to the relation $t = z/v_z$. Now using the fact that $\lambda_P = h/p_z$ and substituting in Equation (3) we get

$$\left(\frac{\partial^2}{\partial x^2} + \frac{\partial^2}{\partial y^2} + i4\pi \frac{1}{\lambda_P} \frac{\partial}{\partial z} \right) \psi(x, y, t = z/v_z) = 0, \tag{4}$$

where λ_P is the wavelength of particle. As we can see the Equations (2) and (4) are formally identical.

The analogy between classical light waves and matter waves is more apparent if we use the formalism of operators in the classical approach introduced by Stoler (Stoler, 1981). In this formalism, the function $A(x,y,z)$ is represented by the ket vector $|A(z)\rangle$. If we take the inner product with the basis vectors $|x,y\rangle$, we obtain $A(x,y,z) = \langle x,y|A(z)\rangle$. The differential operators $-i(\partial/\partial x)$ and $-i(\partial/\partial y)$ acting on the space of functions containing $A(x,y,z)$ are represented in the space of abstract ket by the operators $\hat{k}_x$ and $\hat{k}_y$. The algebraic structure of operators $\hat{k}_x$, $\hat{k}_y$, $\hat{x}$ and $\hat{y}$ is specified by the following commutation relations

$$[\hat{x},\hat{k}_x] \equiv \hat{x}\hat{k}_x - \hat{k}_x\hat{x} = i, \quad [\hat{y},\hat{k}_y] = i, \quad [\hat{x},\hat{y}] = [\hat{x},\hat{k}_y] = [\hat{y},\hat{k}_x] = 0. \tag{5}$$

2.1 The generalized uncertainty relation for light waves

The analogy between the above equations in what concerns the uncertainty relation can be immediately constructed given the formal analogy between the equations.
Consider the plane wave expansion of the normalized wave $u(x,t)$ in one dimension (Jackson, 1999)

$$u(x,t) = \frac{1}{\sqrt{2\pi}} \int dk_x \; A(k_x) e^{i[k_x x - \omega(k_x)t]}. \tag{6}$$

The amplitudes $A(k_x)$ are determined by the Fourier transform of the $u(x,0)$ ($t = 0$ for simplicity)

$$A(k_x) = \frac{1}{\sqrt{2\pi}} \int dx \; u(x,0) e^{-ik_x x}. \tag{7}$$

The averages of functions $f(x,k_x)$ of x and k_x are evaluated as (Stoler, 1981)

$$\langle f(x,k_x)\rangle = \int dx \; u^*(x,0) f_s\left(x, -i\frac{\partial}{\partial x}\right) u(x,0), \tag{8}$$

in complete analogy with quantum mechanics. The function $f_s\left(x, -i\frac{\partial}{\partial x}\right)$ is obtained from $f(x,k_x)$ substituting the c-number variable k_x by the operator $-i\frac{\partial}{\partial x}$ followed by symmetric ordering. For example, if $f(x,k_x) = xk_x$, then $f_s(x, -i\frac{\partial}{\partial x}) = -\frac{i}{2}\left(x\frac{\partial}{\partial x} + \frac{\partial}{\partial x}x\right)$. Thus, we can write the variances

$$\sigma_{xx} = \langle \hat{x}^2\rangle - \langle \hat{x}\rangle^2, \tag{9}$$

$$\sigma_{k_x k_x} = \langle \hat{k}_x^2\rangle - \langle \hat{k}_x\rangle^2, \tag{10}$$

and the covariance

$$\sigma_{xk_x} = -\frac{i}{2} \int dx \; u^*(x) \left(x\frac{\partial}{\partial x} + \frac{\partial}{\partial x}x\right) u(x) - \langle \hat{x}\rangle\langle \hat{k}_x\rangle, \tag{11}$$

and get

$$\sigma_{xx}\sigma_{k_x k_x} - \sigma_{xk_x}^2 \geq \frac{1}{4}. \tag{12}$$

Equation (12) is the equivalent of generalized Schrödinger-Robertson uncertainty relation but for paraxial waves. It is also true in this context that the evolution given by Equation (2) preserves this quantity. This fact allows us to experimentally assess the covariance σ_{xk_x} by the measurements of σ_{xx} and $\sigma_{k_x k_x}$, which are quite simple to perform. Moreover, as we show next, σ_{xk_x} is directly related to the Rayleigh length and Gouy phase.

Next, we show one important result which is a consequence of this analogy - the Gouy phase for matter waves. The free time evolution of an initially Gaussian wave packet

$$\psi(x,y,0) = \left(\frac{1}{b_0\sqrt{\pi}}\right) \exp\left(-\frac{x^2+y^2}{2b_0^2}\right), \tag{13}$$

according to Schrödinger's equation is given by (da Paz, 2006)

$$\psi(x,y,t) = \left[\frac{1}{B(t)\sqrt{\pi}}\right] \exp\left(-\frac{x^2+y^2}{2B^2(t)}\right) \times \exp\left\{i\left[\frac{m\left(x^2+y^2\right)}{2\hbar R(t)} + \mu(t)\right]\right\}. \tag{14}$$

The comparison with the solution of the wave equation in the paraxial approximation with the same condition at $z = 0$ yields

$$w(z) \longrightarrow B(t) = b_0\left[1+\left(\frac{t}{\tau_0}\right)^2\right]^{\frac{1}{2}}, \tag{15}$$

$$R(z) \longrightarrow R(t) = t\left[1+\left(\frac{\tau_0}{t}\right)^2\right], \tag{16}$$

$$\zeta(z) \longrightarrow \mu(t) = -\arctan\left(\frac{t}{\tau_0}\right), \tag{17}$$

and

$$z_0 \longrightarrow \tau_0 = \frac{mb_0^2}{\hbar}. \tag{18}$$

The parameter $B(t)$ ($w(z)$) is the width of the particle beam (of light beam), the parameter $R(t)$ ($R(z)$) is the radius of curvature of matter wavefronts (wavefront of light), $\mu(t)$ ($\xi(z)$) is the Gouy phase for matter waves (for light waves). The parameter τ_0 is only related to the initial condition and is responsible for two regimes of growth of the beam width $B(t)$ (da Paz, 2006; Piza, 2001), in complete analogy with the Rayleigh length which separates the growth of the beam width $w(z)$ in two different regimes as is well known in optics (Saleh & Teich, 1991).
The above equations show that the matter wave propagating in time with fixed velocity in the propagation direction and the stationary electric field in the paraxial approximation are formally identical [if one replaces $t = z/v_z$ in the Equations (15–17)].
Next we show that $\mu(t)$ is directly related to the Schrödinger-Robertson generalized uncertainty relation. For quadratic unitary evolutions (as the free evolution in the present case) the determinant of the covariance matrix is time independent and for pure Gaussian states saturates to its minimum value,

$$\det\begin{pmatrix}\sigma_{xx} & \sigma_{xp}\\ \sigma_{xp} & \sigma_{pp}\end{pmatrix} = \frac{\hbar^2}{4} \tag{19}$$

where

$$\sigma_{xx} = \frac{B(t)^2}{2},\ \sigma_{pp} = \frac{\hbar^2}{2b_0^2}, \tag{20}$$

and

$$\sigma_{xp} = \frac{\hbar t}{2\tau_0} = -\frac{\hbar}{2}\tan 2\mu(t). \tag{21}$$

Since the covariance σ_{xp} is non-null if the Gaussian state exhibits squeezing (Souza et al., 2008), if one measures σ_{xp}, from the above relation it is possible to infer the Gouy phase for a matter wave which can be described by an evolving coherent wave packet. For light waves this is a simple task as can be seen below.

2.2 The Gouy phase for light waves

The generalized uncertainty relation for the Gaussian light field can be immediately obtained. Indeed the variances

$$\sigma_{xx} = \frac{w^2(z)}{4}, \tag{22}$$

$$\sigma_{k_x k_x} = \frac{k}{2z_0}, \tag{23}$$

$$\sigma_{xk_x} = \frac{z}{2z_0} = -\frac{1}{2}\tan 2\zeta(z), \tag{24}$$

satisfy the equality

$$\sigma_{xx}\sigma_{k_x k_x} - \sigma_{xk_x}^2 = \frac{1}{4}. \tag{25}$$

Analogue expressions can be found for the second moments of the y transverse component. The saturation at the value $1/4$ allows for the determination of the covariance σ_{xk_x}. From Equation (25) and using the expressions (22) and (23) we get

$$\sigma_{xk_x}(z) = \pm\frac{1}{2}\sqrt{\left[\frac{w(z)}{w_0}\right]^2 - 1}, \tag{26}$$

which is a function of z/z_0 just like expression (17) for the Gouy phase.

The connection between the Gouy phase and the covariance σ_{xk_x} is of purely kinematical nature. As pointed by Simon and Mukunda (Simon & Mukunda, 1993), the parameter space of the gaussian states has a hyperbolic geometry, and the Gouy phase has a geometrical interpretation related to this geometry.

Note that σ_{xk_x} can be positive or negative according to the Equation (26). However, the Equation (26) was deduced assuming that the focus of the beam is $z = 0$. If we shift the focus to any position z_c, as in the experiment, we must take this into account. The plus and minus sign in Equation (26) can be better understood if we look at the Equation (24)

$$\sigma_{xk_x} = \frac{z}{2z_0} \rightarrow \sigma_{xk_x} = \frac{z - z_c}{2z_0}, \tag{27}$$

which agrees with the experimental data as we show in what follows. Here we can see that for light waves propagating in the direction of focus ($z < z_c$) the covariance is negative, on the other hand, for light waves propagating after focus ($z > z_c$) the covariance is positive.

Now note Equation (26) suggests that by measuring the beam width $w(z)$ we can indirectly infer the value of σ_{xk_x} and thus the value of the Gouy phase by Equation (24). Next, we describe a simple experiment to measure $w(z)$. To experimentally obtain the beam width as a function of the propagation distance, we use the following experimental arrangement shown in Figure 1 (Laboratory of Quantum Optics at UFMG), where L_1 represents a divergent lens,

L_2 a convergent lens and D is a light detector. With this arrangement we can measure the width of the beam as a function of z. The width of the beam in position z is the width of the intensity curve, adjusted by a Gaussian function. In Figure 2, we show the width of the beam for different distances z, along with the corresponding result for σ_{xk_x}.

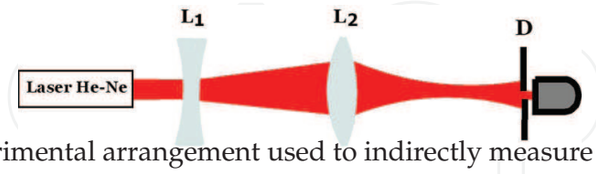

Fig. 1. Sketch of experimental arrangement used to indirectly measure the Gouy phase of a focused light beam.

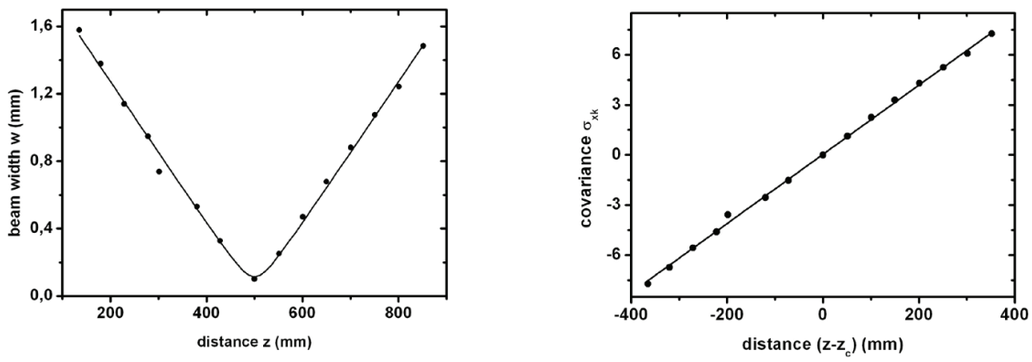

Fig. 2. On the left, the width of Gaussian beam $w(z)$ as a function of propagation direction z. Solid curve corresponds to the Equation (15) and the points were obtained of experiment. On the right, covariance σ_{xk_x} as a function of $z - z_c$. Solid curve corresponds to the Equation (27) and the points were obtained of experiment through the equation (26).

The determination of σ_{xk_x} or $w(z)$ allows us to determine $\xi(z)$ (see Figure 3).

3. Macromolecules diffraction and indirect evidence for the Gouy phase for matter waves

Recent experiments involving the diffraction of fullerene molecules and the uncertainty relation are shown to be quantitatively consistent with the existence of a Gouy phase for matter waves (da Paz et al., 2010). In Ref. (Nairz et al., 2002) an experimental investigation of the uncertainty relation in the diffraction of fullerene molecules is presented. In that experiment, a collimated molecular beam crosses a variable aperture slit and its width is measured as a function of the slit width. Before reaching the slit diffraction the molecular beam passes through a collimating slit whose width is fixed at $\sigma_0 = 10\ \mu m$, producing a correlated beam (see Figures 1 and 3 in Ref. (Nairz et al., 2002)).
The wave function of the fullerene molecules that leave the slit of width b_0, in the transverse direction, is given by

$$\psi_{k_x}(\bar{x}, 0) = \frac{1}{\sqrt{b_0\sqrt{\pi}}} \exp(-\frac{\bar{x}^2}{2b_0^2} + ik_x\bar{x}), \tag{28}$$

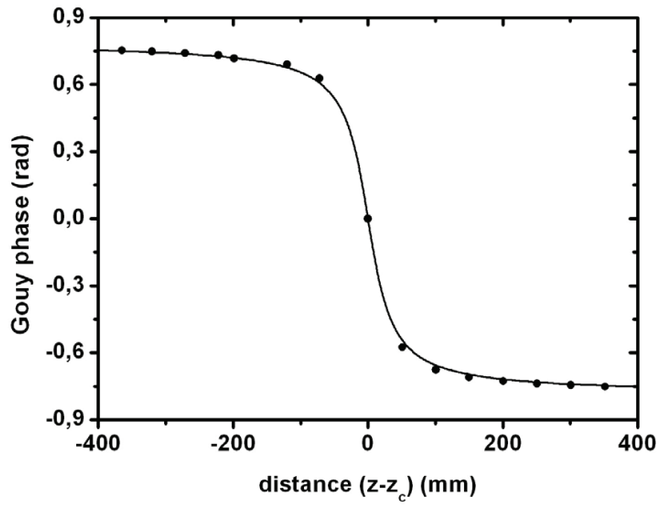

Fig. 3. Gouy phase for Gaussian light beam as a function of propagation direction $z - z_c$. Solid curve corresponds to the Equation (17) and the points were obtained of experiment through the Equation (24).

where k_x is the transverse wave number. The wave function on the screen is given by

$$\psi_{k_x}(x,t) = \int d\bar{x} G(x,t;\bar{x},0)\psi_{k_x}(\bar{x},0), \tag{29}$$

where

$$G(x,t;\bar{x},0) = \left(\frac{m}{2\pi i\hbar t}\right)^{\frac{1}{2}} \exp\left[\frac{im}{2\hbar t}(x-\bar{x})^2\right], \tag{30}$$

and $t = z/v_z$ is the propagation time from slit to detector, v_z is the most probable speed on the z direction. After some algebraic manipulations we obtain, for the normalized wave function at the detector, the following result

$$\psi_{k_x}(x,t) = \frac{1}{\sqrt{\sqrt{\pi}B(t)}} \exp\left[-\frac{1}{2B^2(t)}\left(x - \frac{b_0^2 t}{\tau_0}k_x\right)^2\right] \times \exp\left[\frac{i\mu(t)}{2} + \frac{im}{2\hbar R(t)}\left(x^2 - b_0^4 k_x^2 + \frac{2mb_0^4}{\hbar t}xk_x\right)\right], \tag{31}$$

where $B(t)$, $R(t)$ and $\mu(t)$ are given by the Equations (15), (16) and (17), respectively.
As discussed in Ref. (Viale et al., 2003), given the way the fullerene molecules are produced, it is reasonable to assume that the outgoing beam after the diffraction slit has a random transverse momentum. Due to the thermal production the beam contains different components k_x, although it has been collimated (Viale et al., 2003). The beam is an incoherent mixture of wave functions with wavenumber k_x randomly distributed according to probability distribution $\widetilde{\mathbf{g}}^{(0)}(k_x)$. This distribution depends on the geometry of the collimator, secondary source, which reduces the beam width in the direction x. The index 0 represents the plane of the secondary source (the plane of the collimator), which means that the loss

of coherence of the beam is due to the production mechanism only. It is not physically reasonable to assume that a coherent wave packet leaves the diffraction slit due to the thermal production of the fullerene molecules as discussed above. Therefore, in order to introduce some incoherence along the spatial transverse direction, where the quantum effects occur, we use the formalism of density matrices (Gase, 1994; Ballentine, 1998; Scully & Zubairy, 1997; Fano, 1957). The density matrix of the beam at time t is given by

$$\rho(x,x',t) = \int dk_x \widetilde{\mathbf{g}}^{(0)}(k_x)\psi_{k_x}(x,t)\psi^*_{k_x}(x',t). \tag{32}$$

For simplicity, let us take a probability distribution of wave number k_x be a Gaussian function centered at $k_x = 0$ and width $\Delta k_x = \delta_{k_x}/\sqrt{2}$, i.e.,

$$\widetilde{\mathbf{g}}^{(0)}(k_x) = \frac{1}{\sqrt{\pi}\delta_{k_x}} \exp\left(-\frac{k_x^2}{\delta_{k_x}^2}\right). \tag{33}$$

This allows us to obtain for the density matrix Equation (32), the following result

$$\rho(x,x',t) = \frac{1}{\sqrt{\pi}\bar{B}(t)} \exp\left[-\frac{(x+x')^2 + \mathcal{M}_P^4(x-x')^2}{4\bar{B}^2(t)}\right] \exp\left[\frac{im}{2\hbar\bar{R}(t)}(x^2 - x'^2)\right], \tag{34}$$

where

$$\bar{B}(t) = b_0\left[1 + \left(\frac{t}{\bar{\tau}_0}\right)^2\right]^{\frac{1}{2}},\ \bar{R}(t) = t\left[1 + \left(\frac{\bar{\tau}_0}{t}\right)^2\right], \tag{35}$$

$$\bar{\tau}_0 = \mathcal{M}_P^{-2}\tau_0,\ \mathcal{M}_P^2 = \sqrt{1 + b_0^2\delta_{k_x}^2}. \tag{36}$$

We observe that the density matrix Equation (34) is a mixed state due to the incoherence of the source. The bar has been used to differentiate the parameters of the pure Gaussian state of matter waves of the respective parameters from a mixed Gaussian state. The quantity $\mathcal{M}_P^2$ is the quality factor of the particle beam. The quantity $\bar{\tau}_0$ is a generalization of the definition of time aging (Piza, 2001) (timescale) for partially coherent Gaussian state of matter waves. We see that this quantity is always smaller than the aging time of Gaussian pure states, τ_0, and in this case, a mixed Gaussian state will spread faster with time than the pure Gaussian states. In the coherent limit $\delta_{k_x} \to 0$ (ideal collimation), we obtain the parameters of pure Gaussian state, Equations (15), (16) and (17).
In the limit $t \to 0$ (the plane of source), we have

$$\rho^{(0)}(x,x') = \frac{1}{\sqrt{\pi}b_0} \exp\left[-\frac{(x^2 + x'^2)}{2b_0^2}\right] \exp\left[-\frac{\delta_{k_x}^2}{4}(x-x')^2\right], \tag{37}$$

where the last exponential term of this equation make the role of the spectral degree of coherence defined in the theory of optical coherence (Mandel & Wolf, 1995). We see that the dependence of this term with the transverse position appears as the difference between the positions and, in this case, the source of fullerenes is a source of type Schell (Mandel & Wolf, 1995). Again, the source of fullerenes we refer to here is the collimation slit and not the oven. With the density matrix, we obtain the intensity at the detector by using $x = x'$ e $t = z/v_z$, i.e.,

$$I(x,t) = \rho(x,x,t) = \frac{1}{\sqrt{\pi}\bar{B}(t)} \exp\left[-\frac{x^2}{\bar{B}^2(t)}\right]. \tag{38}$$

Next, we calculate the new elements of the covariance matrix and obtain the following results

$$\begin{aligned}\sigma_{xx} &= \langle \hat{x}^2 \rangle = \int dx x^2 \rho(x,x,t) \\ &= \frac{\bar{B}(t)}{2},\end{aligned} \tag{39}$$

$$\begin{aligned}\sigma_{pp} = \langle \hat{p}^2 \rangle &= \int \left[\int dx \psi^*_{k_x}(x',t)(-\hbar^2 \frac{\partial^2}{\partial x^2}) \psi_{k_x}(x,t) \right]_{x=x'} \widetilde{\mathbf{g}}^{(0)}(k_x) dk_x \\ &= \frac{\hbar^2}{2} \frac{\mathcal{M}_P^4}{b_0^2},\end{aligned} \tag{40}$$

and

$$\begin{aligned}\sigma_{xp} = \langle \frac{\hat{x}\hat{p} + \hat{p}\hat{x}}{2} \rangle &= \int \left[\int dx \psi^*_{k_x}(x',t) x (-i\hbar \frac{\partial}{\partial x}) \psi_{k_x}(x,t) \right]_{x=x'} \widetilde{\mathbf{g}}^{(0)}(k_x) dk_x \\ &= \frac{\hbar}{2} \mathcal{M}_P^2 \left(\frac{t}{\bar{\tau}_0} \right).\end{aligned} \tag{41}$$

With these new elements, we obtain the following result for the determinant of covariance matrix

$$\det \begin{pmatrix} \sigma_{xx} & \sigma_{xp} \\ \sigma_{xp} & \sigma_{pp} \end{pmatrix} = \mathcal{M}_P^4 \frac{\hbar^2}{4}. \tag{42}$$

This result shows that the determinant of the covariance matrix remains time independent, but has a different value from $\frac{\hbar^2}{4}$, because now we have an incoherent state.
The experimental result for the width W_{FWHM} (full width at half maximum) at the detector, realized by the group of A. Zeilinger in Ref. (Nairz et al., 2002) is shown in Figure 4 and compared with our theoretical calculation, Equation (39) (where $W_{FWHM} = 2\sqrt{2 \ln 2 \sigma_{xx}}$). The points are experimental data extracted from Ref. (Nairz et al., 2002), the dashed curve is the beam width with incoherence effect and without convolution with the detector and the solid curve takes into account both effects. These curves show that to adjust the experimental points with theoretical model, we take into account the convolution with the detector and the partial coherence of the fullerenes source. To take into account the convolution with the detector, we use a detector width $FWHM$ of order of 12 μm, where we took as reference the value quoted in (Nairz et al., 2002). The parameter that measures the partial coherence in the transverse direction of the beam that best fits the experimental data is given by $\delta_{k_x} = 9.0 \times 10^6 \, \mathrm{m}^{-1}$.
With this value of δ_{k_x} we calculate the initial transverse coherence length, i.e., $\ell_{0x} = \ell_x(t=0)$ and we obtain $\ell_{0x} = (\delta_{k_x}/\sqrt{2})^{-1} \approx 1.3 \times 10^{-7}$ m. As we do not take into account the coupling with the environment in our model, the initial coherence length remains constant in time, i.e., $\ell_x(t) = \ell_{0x}$. To compare the value of the coherence length with the value of the wavelength, we calculate λ_P through the equation $\lambda_P \approx \lambda_z = h/mv_z$ (where $v_z \approx 200$ m/s is the most probable speed) and we obtain $\lambda_P \approx 2.5$ pm. Thus, we have $\ell_{0x} \gg \lambda_P$, and the condition discussed in Ref. (Mandel & Wolf, 1995) for a locally coherent source is guaranteed. Because the source size is much larger than transverse coherence length, i.e., $\sigma_0 \gg \ell_{0x}$, the angle of beam divergence of fullerenes produced in the secondary source (collimation slit) is given by

$$\bar{\theta}_0 \approx \left(\frac{\lambda_P}{\pi} \right) \frac{1}{\ell_{0x}} = 6.1 \ \mu rad, \tag{43}$$

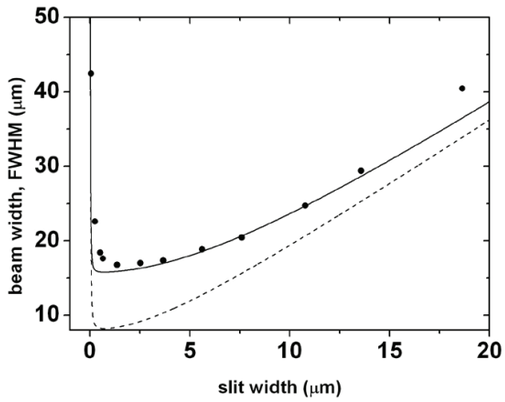

Fig. 4. Beam width of fullerene molecules C_{70} as a function of slit width. Solid and dashed curves correspond to our calculation, Equation (35), and the points are the experimental results obtained in Ref. (Nairz et al., 2002). Dashed curve corresponds to the incoherent case without convolution with the detector and solid curve corresponds to the case where both effects were taken into account. To adjust the theoretical calculation with the experimental data we use $\delta k_x = 9.0 \times 10^6\ \mathrm{m}^{-1}$ and $t = z/v_z = 6.65\,\mathrm{ms}$.

a value consistent with the experimental value quoted in Ref. (Nairz et al., 2000) ($2 \leq \theta \leq 10\ \mu rad$).
The range of wavelengths along the direction x is given by

$$\Delta\lambda_x = \frac{2\pi}{\Delta k_x} = 986\ \mathrm{nm}, \tag{44}$$

where $\Delta k_x = \delta_{k_x}/\sqrt{2} = 6.4 \times 10^6\ \mathrm{m}^{-1}$.
The value obtained for the range of wavelengths is the same order of magnitude of the transverse coherence length ℓ_{0x}, what justifies the existence of quantum effects along this direction. The component of the wave vector in the direction z has the value $k_z = mv_z/\hbar \approx 2.24 \times 10^{12}\ \mathrm{m}^{-1}$. The values found for k_z and Δk_x show that $k_z \gg \Delta k_x$ and thus, paraxial approximation is guaranteed for the partially coherent matter wave beam.

3.1 Covariance σ_{xp} and Gouy phase

In this section, we calculate the covariance between position and momentum and the Gouy phase for fullerenes molecules considering the free Schrödinger equation. We calculate the phase and show that it is also related to the covariance σ_{xp} as well as in the case of pure Gaussian states.
Starting from the determinant of the covariance matrix for mixed Gaussian state, Equation (42), we can express σ_{xp} in terms of the beam width, i.e.,

$$\sigma_{xp} = \frac{\hbar \mathcal{M}_P^2}{2} \left[\left(\frac{W_{FWHM}}{2\sqrt{\ln 2} b_0} \right)^2 - 1 \right]^{\frac{1}{2}}, \tag{45}$$

where W_{FWHM} is measured in the laboratory. The curve for σ_{xp}, obtained with experimental data of the Ref. (Nairz et al., 2002) through the Equation (45), is showed in Figure 5 and compared with the theoretical value, Equation (41).

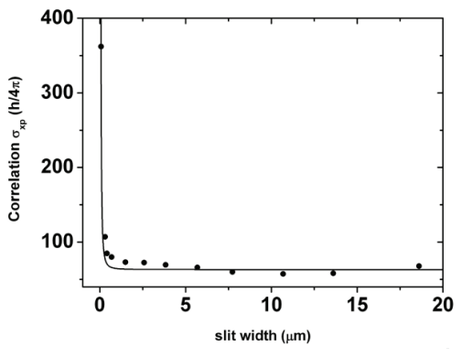

Fig. 5. Covariance σ_{xp} as a function of slit width. Solid curve corresponds to our calculation, Equation (41), and the points were obtained of experiment reported in Ref. (Nairz et al., 2002) through the Equation (45). The parameters are the same of Figure 4.

3.1.1 Gouy phase for a mixed Gaussian state

A more recent definition justifies the physical origin of the Gouy phase in terms of space enlargement, governed by the uncertainty relation, of a beam whose transverse field distribution is a Gaussian function (or arbitrary) (Feng & Winful, 2001). According to Equation (11) in Ref. (Feng & Winful, 2001) the Gouy phase $\mu(t)$ and the beam width $B(t)$ for a pure Gaussian state of matter waves are related by the expression

$$\mu(t) = -\frac{\hbar}{2m}\int^{t}\frac{dt}{B(t)^2}. \tag{46}$$

Here, we conjecture, based on the obtained results, that this definition holds for partially coherent Gaussian states since the spread of these states is also governed by the uncertainty relation. Thus, for a state given by Equation (34), the Gouy phase is

$$\mu(t) = -\frac{1}{2\mathcal{M}_P^2}\arctan\left(\frac{t}{\bar{\tau}_0}\right), \tag{47}$$

where the factor $\frac{1}{2}$ appears because we are working in one dimension. Note that, again $\mu(t)$ is related to σ_{xp} and is affected by the partial coherence of the initial wave packet, i.e.,

$$\mu(t) = -\frac{1}{2\mathcal{M}_P^2}\arctan\left(\frac{2\sigma_{xp}}{\hbar\mathcal{M}_P^2}\right). \tag{48}$$

In Figure 6, we show the phase extracted from Equation (48). As expected, the variation in phase is $\pi/4$, because we are dealing with a one-dimensional problem of diffraction and the propagation of the beam will be from $t = 0$ to $t = z/v_z$ (Feng & Winful, 2001). This result shows that the existence of a Gouy phase is compatible with the experimental data involving diffraction of fullerene molecules. It is an indirect evidence of the Gouy phase for matter waves (da Paz, 2011; da Paz et al., 2010).

4. Quantum lens and Gouy phase for matter waves

In the previous section, we have shown an indirect evidence for the Gouy phase for matter waves based on the analogy existent between the paraxial equation for wave optics and

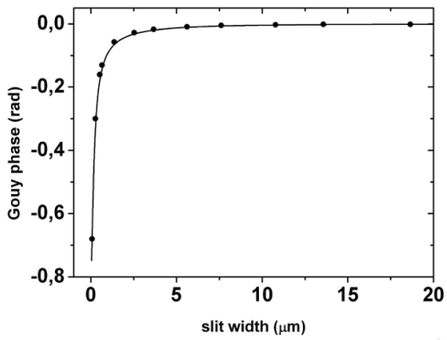

Fig. 6. Gouy phase as a function of slit width. Solid curve corresponds to our calculation, Equation (47), and the points were obtained of experiment reported in Ref. (Nairz et al., 2002). The parameters are the same of Figure 4.

Schrödinger equation for matter waves (da Paz, 2011; da Paz et al., 2010). Due to this formal similarity a question which arises naturally is if a similar phase anomaly may occur in the region around the focus of an atomic beam. In order to answer this question, in this section we present the evolution of an atomic beam described by a Gaussian wave packet interacting dispersively with a cavity field (da Paz, 2011; da Paz et al., 2007).
The model we use is the following (Averbukh etal., 1994; Rohwedder & Orszag, 1996; Schleich, 2001): consider two-level atoms moving along the Oz direction and that they penetrate a region where a stationary electromagnetic field is maintained. The region is the interval $z = -L_c$ until $z = 0$. The atomic linear moment in this direction is such that the de Broglie wavelength associated is much smaller than the wavelength of the electromagnetic field. We assume that the atom moves classically along direction Oz and the atomic transition of interest is detuned from the mode of the electromagnetic field (dispersive interaction). The Hamiltonian for this model is given by

$$\hat{H}_{AF} = \frac{\hat{p}_x^2}{2m} + g(\hat{x})\hat{a}^\dagger\hat{a} \tag{49}$$

where m is the atom mass, $\hat{p}_x$ and $\hat{x}$ are the linear momentum and position along the direction Ox, $\hat{a}^\dagger$ and $\hat{a}$ are the creation and destruction operators of a photon of the electromagnetic mode, respectively. The coupling between atom and field is given by the function $g(x) = \alpha E^2(x)$ where α is the atomic linear susceptibility, $\alpha = \frac{\wp^2}{\hbar\Delta}$, where $\wp^2$ is the square of the dipole moment and Δ is the detuning. $E(x)$ corresponds to the electric field amplitude in vacuum. The effective interaction time is $t_L = \frac{L_c}{v_z}$, where v_z is the longitudinal velocity of the atoms.
The dynamics of the closed system is governed by the Schrödinger equation

$$i\hbar\frac{d}{dt}|\Psi\rangle = \hat{H}_{AF}|\Psi\rangle. \tag{50}$$

At $t = 0$ the state of the system is given by a direct product of the state corresponding to the transversal component of the atom and a field state, $|\Psi_{cm}\rangle \otimes |\Psi_F\rangle$. The field state can be expanded in the eigenstates of the number operator $\hat{a}^\dagger\hat{a}$

$$|\Psi_F\rangle = \sum_n \omega_n|n\rangle, \quad \sum_n |\omega_n|^2 = 1. \tag{51}$$

When atom and field interact the atomic and field states get entangled. We can then write

$$|\Psi(t)\rangle = \sum_n \omega_n \int_{-\infty}^{+\infty} dx\, \psi_n(x,t)|x\rangle \otimes |n\rangle\,, \tag{52}$$

where

$$i\hbar \frac{\partial}{\partial t}\psi_n(x,t) = \left\{-\frac{\hbar}{2m}\nabla^2 + g(x)n\right\}\psi_n(x,t)\,, \tag{53}$$

or, if one defines

$$|\Psi_n(t)\rangle = \int_{-\infty}^{+\infty} dx\, \psi_n(x,t)|x\rangle\,, \tag{54}$$

the Equation (53) takes the form

$$i\hbar \frac{d}{dt}|\Psi_n(t)\rangle = \left[\frac{\hat{p}_x^2}{2m} + g(\hat{x})n\right]|\Psi_n(t)\rangle. \tag{55}$$

Next, we will use the harmonic approximation for $g(x)$ which is a fine approximation provided the dispersion of the wavepacket in the transverse direction b_0 is much smaller than the wavelength of the electromagnetic field mode λ (Schleich, 2001). Taking the main terms of the Taylor expansion of the function $g(x)$,

$$g\,(x) \approx g_0 - \frac{g_1^2}{2g_2} + \frac{1}{2}g_2\left(x - x_f\right)^2\,, \tag{56}$$

we get

$$\begin{aligned} i\hbar \frac{d}{dt}|\Psi_n(t)\rangle &= \left[\frac{\hat{p}_x^2}{2m} + \frac{1}{2}m\Omega_n^2(\hat{x} - x_f)^2\right]|\Psi_n(t)\rangle \\ &\equiv \hat{H}_n|\Psi_n(t)\rangle\,, \end{aligned} \tag{57}$$

where $x_f = -g_1/2g_2$ and $\Omega_n^2 = ng_2/m$. In order to obtain focalization of the atomic beam it is crucial that the initial state be compressed in momentum since this initial momentum compression is transferred dynamically to the x coordinate and a focus can be obtained (da Paz et al., 2007; Rohwedder & Orszag, 1996). In fact, the momentum compression is a necessary condition in optics to obtain a well defined focus (Saleh & Teich, 1991).

4.1 Time evolution

According to Bialynicki-Birula (Bialynicki-Birula, 1998), the general form of a Gaussian state in the position representation, is given by

$$\psi\,(x) = \left(\frac{u}{\pi}\right)^{\frac{1}{4}} \exp\left(-i\frac{\bar{x}\bar{p}}{2\hbar}\right) \exp\left[-\frac{(x-\bar{x})^2\,(u+iv)}{2} + i\frac{\bar{p}x}{\hbar}\right], \tag{58}$$

where $\bar{x}$ and $\bar{p}$ are the coordinates of "center of mass" of the distribution in phase space and u and v give the form of this distribution.

A dynamic governed by a Hamiltonian quadratic in position and momentum keep the Gaussian shape of a Gaussian initial state. This is the case of the problem treated here. The atomic motion can be divided into two stages: the first, the atom undergoes the action of a harmonic potential when it crosses the region of electromagnetic field while, in the second

part, the atom evolves freely. In the two stages, the Hamiltonian governing the evolution are quadratic in atomic position and momentum [*cf.* Equation (57)]. Since the initial atomic state is Gaussian, we can consider that throughout evolution, such state will preserve the form given by Equation (58). In this case, the parameters $\bar{x}$, $\bar{p}$, u and v are functions of time, and their respective equations of motion can be derived from the Schrödinger equation.
Consider a particle of mass m moving under the action of a harmonic potential. The natural frequency of this movement is Ω_n. The Hamiltonian governing this dynamic is given by

$$\hat{H} = \frac{\hat{p}_x^2}{2m} + \frac{1}{2} m\Omega_n^2 \hat{x}^2. \tag{59}$$

In position representation, the evolution of the state ψ of the particle is governed by the Schrödinger equation

$$i\hbar \frac{\partial}{\partial t}\psi(x,t) = \left[-\frac{\hbar^2}{2m}\frac{\partial^2}{\partial x^2} + \frac{1}{2} m\Omega_n^2 x^2 \right] \psi(x,t). \tag{60}$$

Suppose that the initial state of the particle is Gaussian. We obtain the equations of motion for the parameters $\bar{x}$, $\bar{p}$, u and v by substituting the general form (58) in equation above, grouping the terms of same power in $(x - \bar{x})$, and then separating the real and imaginary parts. This procedure takes six equations for the four parameters mentioned. The system is therefore, "super-complete". Eliminating such redundancy, the equations of motion are the following

$$\dot{\bar{x}} = \frac{\bar{p}}{m}\,, \tag{61a}$$

$$\dot{\bar{p}} = -m\Omega_n^2 \bar{x}\,, \tag{61b}$$

$$\dot{K} = i\frac{m\Omega_n^2}{\hbar} - i\frac{\hbar}{m}K^2\,, \tag{61c}$$

where we define $K = u + iv$. Here, the dots indicate time derivation. Note that the equations of motion for the coordinates of the centroid of the distribution are equivalent to the classical equations of movement to the position and momentum of a particle moving in a harmonic potential.
A important observation must be made here. One of the two equations removed is not consistent with the others in (61). This equation is the following:

$$\bar{p}\dot{\bar{x}} - \dot{\bar{p}}\bar{x} = \frac{\bar{p}^2}{m} + m\Omega_n^2 \bar{x}^2 + \frac{\hbar^2}{m} u. \tag{62}$$

To see this, just replace the expressions (61a), (61b) in the above equation. We obtain $u = 0$, which makes no sense, since u represents the inverse square of the width of the Gaussian package. The only way to "dribble" this inconvenience is to redefine the general state as

$$\psi(x) = \left(\frac{u}{\pi}\right)^{\frac{1}{4}} \exp\left(-i\frac{\bar{x}\bar{p}}{2\hbar} + i\frac{\Phi}{2}\right) \exp\left[-\frac{(x-\bar{x})^2 (u+iv)}{2} + i\frac{\bar{p}x}{\hbar} \right], \tag{63}$$

where Φ is a real function of time. This global phase, in general neglected (see, e.g., (Bialynicki-Birula, 1998; Piza, 2001)), ensures the consistency of the equations of motion because, in addition to Equations (61), we must have

$$\dot{\Phi} = -\frac{\hbar}{m} u. \tag{64}$$

$\Phi/2$ is known as *Gouy phase*. Equation (64) relates the Gouy phase with the inverse square of the beam width . The same result was obtained for light waves transversally confined in Ref. (Feng & Winful, 2001).

4.2 Focalization of the atomic beam

In Figure 7 we illustrated how the quantum lens work out. We consider that a initial Gaussian state compressed in the momentum (region I) penetrates in a region where a stationary electromagnetic field is maintained (region II). The atoms and the field inside the cavity interact dispersively. Dispersive coupling is actually necessary to produce a quantum lens, because the transitions cause aberration at the focus (Berman, 1997; Rohwedder & Orszag, 1996; Schleich, 2001). When the atomic beam leaves the region of the electromagnetic field, the atomic state evolves freely and the compression is transferred to the position (region III). Let us assume, as an initial atomic state, the compressed vacuum state

$$\langle x|\psi_n(t=0)\rangle = \psi_n(x,t=0) = \left(\frac{1}{b_0\sqrt{\pi}}\right)^{1/2} \exp\left(-\frac{x^2}{2b_0^2}\right), \tag{65}$$

where b_0 is the initial width of the packet and $b_0 > b_n = \sqrt{\hbar/\left(m\Omega_n\right)}$. For the parameters $\bar{x}$,

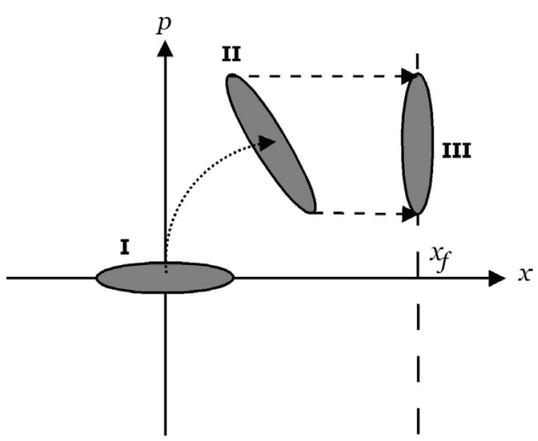

Fig. 7. Initial atomic compressed state in momentum . The evolution inside the cavity rotates the state and transfer the compression to the position.

$\bar{p}$, K and Φ, we get

$$\bar{x}(t<t_L) = -x_f \cos\Omega_n t\,, \tag{66}$$

$$\bar{p}(t<t_L) = m\Omega_n x_f \sin\Omega_n t\,, \tag{67}$$

and

$$K(t<t_L) = \left(\cos\Omega_n t + i\frac{b_n^2}{b_0^2}\sin\Omega_n t\right)^{-1}\left(\frac{1}{b_0^2}\cos\Omega_n t + i\frac{1}{b_n^2}\sin\Omega_n t\right), \tag{68}$$

for the initial conditions $\bar{x}_0 = -x_f, \bar{p}_0 = 0, u = b_0^{-2}$ and $v = 0$. Also, from Equation (68) we obtain

$$u(t<t_L) = \left[b_0^2\left(\cos^2\Omega_n t + \frac{b_n^4}{b_0^4}\sin^2\Omega_n t\right)\right]^{-1}. \tag{69}$$

Now u^{-1} is the width of the gaussian wavepacket squared. At this stage

$$\Phi(t < t_L) = -\frac{1}{\Omega_n \tau_n} \arctan\left[\frac{b_n^2}{b_0^2}\tan(\Omega_n t)\right]. \tag{70}$$

When the atomic beam leaves the region of the electromagnetic field, the atomic state evolves freely. The equations of motion can be obtained analogously and we get for $t > t_L$

$$\bar{x}(t > t_L) = -x_f \cos\phi_n + \Omega_n (t - t_L) x_f \sin\phi_n, \tag{71}$$

$$\bar{p}(t > t_L) = m\Omega_n x_f \sin\phi_n, \tag{72}$$

$$K(t > t_L) = \frac{\frac{b_n^2}{b_0^2}\cos\phi_n + i\sin\phi_n}{b_n^2\left[\cos\phi_n + i\frac{b_n^2}{b_0^2}\sin\phi_n + i\frac{t-t_L}{\tau_n}\left(\frac{b_n^2}{b_0^2}\cos\phi_n + i\sin\phi_n\right)\right]} \tag{73}$$

and

$$b_0^2 u(t > t_L) = \left[\left(\cos\phi_n - \frac{t-t_L}{\tau_n}\sin\phi_n\right)^2 + \frac{b_n^4}{b_0^4}\left(\sin\phi_n + \frac{t-t_L}{\tau_n}\cos\phi_n\right)^2\right]^{-1}, \tag{74}$$

where $\phi_n = \Omega_n t_L$ and $\tau_n = m b_n^2/\hbar$.
The focus will be located in the atomic beam region where the width of the wavepacket is minimal. In other words, when $u(t > t_L)$ be a maximum there will be the focus. This will happen when the function

$$D(t) = \left(\cos\phi_n - \frac{t-t_L}{\tau_n}\sin\phi_n\right)^2 + \frac{b_n^4}{b_0^4}\left(\sin\phi_n + \frac{t-t_L}{\tau_n}\cos\phi_n\right)^2 \tag{75}$$

attains its minimum value. The time for which its derivative vanishes is given by

$$t_f = \frac{z_f + L_c}{v_z} = t_L + \tau_n \frac{\left(1 - \frac{b_n^4}{b_0^4}\right)^2 \sin\phi_n \cos\phi_n}{\frac{b_n^4}{b_0^4}\cos^2\phi_n + \sin^2\phi_n}, \tag{76}$$

therefore the focus is located at

$$z_f = v_z \tau_n \frac{\left(1 - \frac{b_n^4}{b_0^4}\right)\tan\phi_n}{\frac{b_n^4}{b_0^4} + \tan^2\phi_n}. \tag{77}$$

The width of the Gaussian beam that passed through the lens, $B'(t) = 1/\sqrt{u(t)}$, can be written as

$$B'(t) = b_0'\left[1 + \left(\frac{t - t_f}{\tau_0'}\right)^2\right]^{\frac{1}{2}} \tag{78}$$

where we define

$$b_0' = M b_0, \tag{79}$$

$$\tau_0' = M^2 \tau_0, \tag{80}$$

and

$$M = \frac{1}{\sqrt{\cos^2\phi_n + \frac{b_0^4}{b_n^4}\sin^2\phi_n}}. \tag{81}$$

The line was used here to differentiate the beam parameters after the focalization of their parameters before the focalization. We see that the waist of the beam is increased by factor M and the package time aging is increased by the M^2 (not confuse with the quality factor $\mathcal{M}_P$). In optics, the amount M is known as magnification factor (Saleh & Teich, 1991). If the state is not initially compressed, i.e., if $b_n = b_0$, does not exist focalization and in this case $b_0' = b_0$ and $\tau_0' = \tau_0$ as we can seen by the Equations (79), (80) and (81).
If we consider an interaction time of atoms with cavity field t_L very small, we have the so called thin lens regime. Because when the interaction time is very small, the movement of atoms along the transverse direction is also very small, i.e., the average transverse kinetic energy of atoms is much smaller than the average potential energy $\langle\hat{U}(x)\rangle$ produced by field, $\frac{\langle\hat{p}_x^2\rangle}{2m} \ll \langle\hat{U}(x)\rangle$ (Averbukh etal., 1994). The rotation angle of the atomic state caused by the interaction with the cavity field $\phi_n = \Omega_n t_L$ is directly proportional to the interaction time, thus, if t_L is too small, ϕ_n will also be very small. If we consider $\phi_n \ll 1$ and an initial atomic state compressed in the momentum with $b_n/b_0 \ll 1$, the expression for the focal distance, equation (77), acquires the simple form (Schleich, 2001)

$$z_f = \frac{mv_z^2}{ng_2 L_c}. \tag{82}$$

4.3 Phase anomaly

If we integrate the equation of motion (64) for Φ considering the expression for $B'(t)$ given by the Equation (78), we obtain

$$\begin{aligned}\mu(t) = \frac{\Phi(t)}{2} &= -\frac{\hbar}{2m}\int_{t_f}^{t}\frac{dt}{B'^2(t)} \\ &= -\frac{1}{2}\arctan\left(\frac{t-t_f}{\tau_0'}\right).\end{aligned} \tag{83}$$

The integration interval is taken from t_f to t, because the Gouy phase is the phase of the Gaussian state relatives to the plane wave at the focus, i.e., at the focus the Gaussian state is in phase with the plane wave (Saleh & Teich, 1991; Boyd, 1980; Feng & Winful, 2001). At the focus, $\mu = 0$, as expected. Therefore, the Gouy phase of the atomic wave function undergoes a change of $\pi/2$ near the focus t_f. The fact that this variation is only $\pi/2$, in contrast with the value of π for the light, is due to the fact that the quantum lens focuses the atomic beam in the Ox direction, keeping the Oy direction unperturbed (i.e., the electromagnetic field acts as a cylindrical lens).

5. Experimental proposal

Consider a Rydberg atom with a level structure given in Figure 8 (left). Three Rydberg levels e, g, and i are taken into account. The transition between the states e and g is slightly detuned with a stationary microwave field stored in two separated cavities with frequency ω, C_1 and C_2, and completely detuned with the transition $g \to i$. These cavities are placed between two Ramsey zones, R_1 and R_2, where a microwave mode quasi-resonant with the atomic transition

$g \rightarrow i$ is stored (see Figure 8). If the electronic atomic state involve the levels i or g, the field in both Ramsey zones are adjusted to imprint a $\pi/2$ Rabi pulse on the internal state of the atom. Then, after the Ramsey zones, the electronic state changes as

$$|i\rangle = \frac{1}{\sqrt{2}}(|i\rangle + |g\rangle) \tag{84}$$

and

$$|g\rangle = \frac{1}{\sqrt{2}}(|i\rangle - |g\rangle). \tag{85}$$

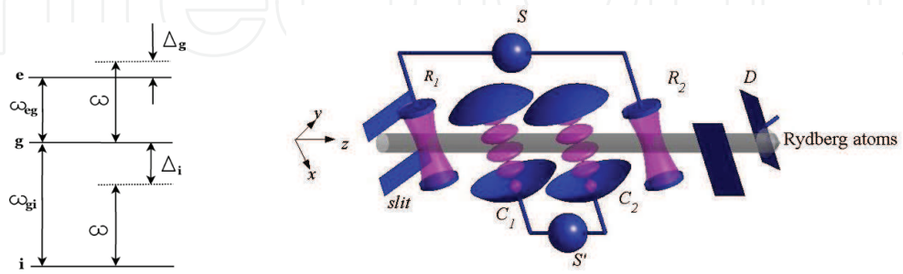

Fig. 8. On the left, atomic energy levels compared with the wavelength of the field inside the cavities C_1 and C_2. On the right, sketch of the experimental setup to measure the Gouy phase for matter waves. Rydberg atoms are sent one-by-one with well-defined velocity along the z-axis. A slit is used to collimate the atomic beam in the x-direction. The Ramsey zones R_1 and R_2 are two microwave cavities fed by a common source S, whereas C_1 and C_2 are two high-Q microwave cavities devised to work as thin lenses for the atomic beam. The field inside these cavities is supplied by common source S'. The state of each atom is detected by the detector D.

The experimental setup we propose to measure the Gouy phase shift of matter waves is depicted in Figure 8 (right). This proposal is based on the system of Ref. (Raimond et al., 2001). Rubidium atoms are excited by laser to a circular Rydberg state with principal quantum number 49 (Nussenzveig et al., 1993; Gallagher, 1994), that will be called state $|i\rangle$, and their velocity on the z direction is selected to a fixed value v_z. As it was stated before, we will consider a classical movement of the atoms in this direction, with the time component given by $t = z/v_z$. A slit is used to prepare a beam with small width in the x direction, but still without a significant divergence, such that the consideration that the atomic beam has a plane-wave behaviour is a good approximation.

If we disregard the cavities C_1 and C_2, the setup is that of an atomic Ramsey interferometer (Ramsey, 1985). The cavity R_1 has a field resonant or quasi resonant with the transition $|i\rangle \Leftrightarrow |g\rangle$ and results in a $\pi/2$ pulse on the atoms, that exit the cavity in the state $(|i\rangle + |g\rangle)/\sqrt{2}$ (Raimond et al., 2001; Ramsey, 1985; Kim et al., 1999; Gerry & Knight, 2005). After passing through the cavity R_1, the atoms propagate freely for a time t until the cavity R_2, that also makes a $\pi/2$ pulse on the atoms. Calling $\hbar\omega_g$ and $\hbar\omega_i$ the energy of the internal states $|g\rangle$ and $|i\rangle$ respectively, ω_r the frequency of the field in the cavities R_1 and R_2 and defining $\omega_{gi} \equiv \omega_g - \omega_i$, the probability that detector D measures each atom in the $|g\rangle$ state is (Raimond et al., 2001; Ramsey, 1985; Nogues et al., 1999)

$$P = \cos^2[(\omega_r - \omega_{gi})t] \ . \tag{86}$$

Upon slightly varying the frequency ω_r of the fields in cavities R_1 and R_2, the interference fringes can be seen (Raimond et al., 2001; Ramsey, 1985; Nogues et al., 1999).

5.1 Atom focalization by classical fields

The interaction between a two-level atom and a single mode of the electromagnetic field (EMF) is governed by the semiclassical hamiltonian

$$\hat{H}_{AF} = -\hat{d} \cdot \vec{E}(\hat{\vec{r}}, t). \tag{87}$$

$\hat{d} = \vec{\epsilon}_d \wp \hat{\sigma}_x^{eg}$ is the dipole moment operator, where $\vec{\epsilon}_d$ is the unitary vector along the direction of quantization, $\wp$ is the element of the transition matrix between the levels e (excited) and g (ground state), and $\hat{\sigma}_x^{eg} = |e\rangle\langle g| + |g\rangle\langle e|$. Assuming the longwave approximation, the electric field $\vec{E}$ is considered in the position $\vec{r}$ of the atomic center of mass ($\hat{\vec{r}}$ is the corresponding quantum operator). Here, $\vec{E}$ is treated classically.

Let us suppose that the atom interacts with a stationary electromagnetic wave kept in a cavity. Moreover, the atom moves along the Oz direction, while the stationary field is formed by two counterpropagating components along the Ox axis and linearly polarized in the direction Oy. We have

$$\vec{E}(\hat{\vec{r}}, t) = \vec{\epsilon}_y [E_0 \, e^{i(k\hat{x} - \omega t)} + E_0 \, e^{i(k\hat{x} + \omega t)} + h.c], \tag{88}$$

where E_0 is a complex amplitude. Thus, we can write

$$\vec{E}(\hat{\vec{r}}, t) = \vec{\epsilon}_y [2E_0 \, e^{ik\hat{x}} \cos(\omega t) + h.c]. \tag{89}$$

Here, $k = \frac{2\pi}{\lambda}$, where λ is the wavelength of the EMF, and h.c. stands for hermitean conjugate. Without loss of generality, we can take E_0 real. Hence,

$$\vec{E}(\hat{\vec{r}}, t) = 4\vec{\epsilon}_y E_0 \cos(k\hat{x}) \cos(\omega t). \tag{90}$$

Assuming $\vec{\epsilon}_y = \vec{\epsilon}_d$, we have

$$\hat{H}_{AF} = -4pE_0 \cos(k\hat{x}) \cos(\omega t) \hat{\sigma}_x^{eg} \equiv \Omega_0 \cos(k\hat{x}) \cos(\omega t) \hat{\sigma}_x^{eg}, \tag{91}$$

where $|\Omega_0| = 4\wp E_0$ is the Rabi vacuum frequency.

The hamiltonian that governs the atomic dynamics during the interaction with the stationary field is given by

$$\hat{H} = \frac{\hat{P}_x^2}{2m} + \frac{\hbar\omega_{eg}}{2} \hat{\sigma}_z^{eg} + \hbar\Omega_0 \cos(k\hat{x}) \cos(\omega t) \hat{\sigma}_x^{eg}. \tag{92}$$

Here, $\hat{\sigma}_z^{eg} = |e\rangle\langle e| - |g\rangle\langle g|$, and m is the atomic mass. In the rotating wave approximation (RWA), we have

$$\hat{H} = \frac{\hat{P}_x^2}{2m} + \frac{\hbar\omega_{eg}}{2} \hat{\sigma}_z^{eg} + \frac{\hbar\Omega_0}{2} \cos(k\hat{x}) (e^{-i\omega t} |e\rangle\langle g| + e^{i\omega t} |g\rangle\langle e|). \tag{93}$$

In order to remove the temporal dependence of $\hat{H}$, we define $|\tilde{\psi}(t)\rangle = \exp\left(i\frac{\omega t}{2}\hat{\sigma}_z^{eg}\right) |\psi(t)\rangle$. Then, the evolution of the state $|\tilde{\psi}(t)\rangle$ is governed by the equation

$$i\hbar \frac{d}{dt} |\tilde{\psi}\rangle = \hat{\tilde{H}} |\tilde{\psi}\rangle, \tag{94}$$

where

$$\hat{\tilde{H}} = \frac{\hat{P}_x^2}{2m} + \frac{\hbar\Delta}{2} \hat{\sigma}_z^{eg} + \frac{\hbar\Omega_0}{2} \cos(k\hat{x}) \hat{\sigma}_x^{eg}. \tag{95}$$

Here, we define $\Delta = \omega_{eg} - \omega$ as the detuning between the frequency of the atomic transition and the frequency of the field mode. In the limit of thin lens, the kinetic energy term can be neglected. So, we have

$$\hat{\hat{H}} = \frac{\hbar\Delta}{2}\hat{\sigma}_z^{eg} + \frac{\hbar\Omega_0}{2}\cos(k\hat{x})\hat{\sigma}_x^{eg}. \tag{96}$$

Let us define the operator $\hat{\Omega}_x = \Omega_0\cos(k\hat{x})$. Consider the set composed by the states $|e,x\rangle = |e\rangle \otimes |x\rangle$ and $|g,x\rangle = |g\rangle \otimes |x\rangle$, where $|x\rangle$ is an eigenstate of the operator $\hat{x}$ with eigenvalue x. In the basis $\{|e,x\rangle, |g,x\rangle\}_{x\in\mathbb{R}}$, $\hat{\hat{H}}$ is represented by the matrix

$$\hat{\hat{H}}_x = \begin{pmatrix} \Delta & \Omega_x \\ \Omega_x & -\Delta \end{pmatrix}, \tag{97}$$

which is diagonalized by the eigenvectors

$$|+,x\rangle = \frac{\Omega_x}{\sqrt{(\Delta_x-\Delta)^2+\Omega_x^2}}|e,x\rangle + \frac{\Delta_x-\Delta}{\sqrt{(\Delta_x-\Delta)^2+\Omega_x^2}}|g,x\rangle, \tag{98}$$

$$|-,x\rangle = \frac{\Delta_x-\Delta}{\sqrt{(\Delta_x-\Delta)^2+\Omega_x^2}}|e,x\rangle - \frac{\Omega_x}{\sqrt{(\Delta_x-\Delta)^2+\Omega_x^2}}|g,x\rangle. \tag{99}$$

with the following eigenvalues

$$E_{\pm,x} = \pm\frac{\hbar}{2}\Delta_x = \pm\frac{\hbar}{2}\sqrt{\Delta^2+\Omega_x^2}. \tag{100}$$

Here, $\Omega_x = \Omega_0\cos(kx)$ is an eigenvalue of the operator $\hat{\Omega}_x$. In the dispersive limit, we have $\frac{|\Omega_x|}{\Delta} \ll 1$. In this limit, the eigenvectors and the eigenvalues given by the above equations can be approximated by

$$|+,x\rangle \to |e,x\rangle\ ,\ |-,x\rangle \to |g,x\rangle, \tag{101}$$

$$E_{\pm,x} \to \pm\frac{\hbar}{2}\left(\Delta + \frac{\Omega_x^2}{2\Delta}\right). \tag{102}$$

Besides, assuming that the width of the atomic wavepacket is small compared with the wavelength of the stationary EMF (harmonic approximation), $\Omega_x^2 = \Omega_0^2\cos^2(kx)$ can be expanded to $\Omega_x^2 \approx \Omega_{min}^2 + \Omega_0^2k^2x^2$. The fact that we have chosen the point $\pi/2$ to do the expansion means that we are treating the case of blue detuning ($\Delta < 0$), i.e., the case in which the atoms will pass in the region of electric field node (Berman, 1997). Also we define $\Omega_x^2(\pi/2) \equiv \Omega_{min}^2$ to be different of zero, since the potential is produced by fields counterpropagating and it difficultly will be null for real cavities. Thus, taking the dispersive and harmonic approximations, we can define the effective hamiltonian

$$\hat{\hat{H}}_{eff} = \frac{\hbar}{2}\left(\Delta + \frac{\Omega_{min}^2}{2\Delta} + \frac{\Omega_0^2}{2\Delta}k^2\hat{x}^2\right)\hat{\sigma}_z^{eg}. \tag{103}$$

As discussed above, the devised experiment uses three atomic levels and the third level i possesses energy below of the energy of the levels g and e , as shown in Figure 8. The frequencies ω_{gi} and ω_{eg} satisfy $\omega_{gi} > \omega_{eg}$, thus the transition $g \to i$ is very far from the

resonance with the stationary mode. In this case, adopting the same reasoning sketched above, the introduction of this level modifies the effective hamiltonian given in the Equation (103)

$$\hat{H}_{eff} = \frac{\hbar\Delta_i}{2}\hat{\sigma}_z^{gi} + \frac{\hbar}{2}\left(\Delta_g + \frac{\Omega_{min}^2}{2\Delta_g} + \frac{\Omega_0^2}{2\Delta_g}k^2\hat{x}^2\right)\hat{\sigma}_z^{eg}, \tag{104}$$

where $\Delta_i = \omega_{gi} - \omega$, $\Delta_g = \omega_{eg} - \omega$, and $\hat{\sigma}_z^{gi} = |g\rangle\langle g| - |i\rangle\langle i|$. Note that the effective coupling between the atom in the state i and the EMF is neglected in the above hamiltonian.
In order to discuss the focalization, let us consider the following initial state

$$|\tilde{\psi}(0)\rangle = \frac{1}{\sqrt{2}}(|i\rangle + |g\rangle) \otimes \psi_{cm}(x), \tag{105}$$

where $|\psi_{cm}\rangle$ stands for some state of the atomic center of mass coordinate. The atom prepared in this state interacts with the stationary field during a time interval t_L. After this interval, the state of the atom will be given by

$$|\tilde{\psi}(t_L)\rangle = \frac{1}{\sqrt{2}}[e^{i\phi_i}|i\rangle \otimes \psi_{cm}(x) + e^{-i(\phi_i - \phi_g)}|g\rangle \otimes \psi'_{cm}(x)], \tag{106}$$

where $\phi_i = \frac{\Delta_i}{2}t_L$, $\phi_g = \left(\frac{\Delta_g}{2} + \frac{\Omega_{min}^2}{4\Delta_g}\right)t_L$ are the phase shifts accumulated by the electronic levels during the interaction, and

$$\psi'_{cm}(x) = e^{i\frac{k^2\Omega_0^2 t_L}{4\Delta_g}x^2}\psi_{cm}(x) \tag{107}$$

is the evolved state of the center of mass of atomic beam composed of atoms in $|g\rangle$ state. As $\Delta_g < 0$, blue detuning, after to pass through the cavity satisfying the approaches that we use, the center of mass state gets a negative quadratic phase. An optical converging cylindrical lens with focal distance f puts a quadratic phase $-kx^2/(2f)$ on the electromagnetic beam (Saleh & Teich, 1991). By analogy, a thin lens for atoms should put a phase of the type $-k_P x^2/(2f_P)$ in the atomic beam, where $k_P = mv_z/\hbar$ is the atomic wave number and f_P the corresponding focal distance. If we compare this phase with the phase in the Equation (107), we get

$$f_P = \frac{2|\Delta_g|mv_z^2}{L_c\hbar k^2\Omega_0^2}. \tag{108}$$

This expression is the focal distance for a thin classical lens. Different from Equation (82) to thin quantum lens, this expression does not have a explicit dependence with photon number of the field mode.
The Rayleigh range z'_r and the beam waist w'_0 of the focused atomic beam also can be calculated using the analogy with the action of lenses in electromagnetic beams considering that the incident beam has plane wavefronts (Saleh & Teich, 1991)

$$z'_r = \left[\frac{1}{1 + (z_r/f_P)^2}\right] z_r \ , \ w'_0 = \sqrt{\frac{1}{1 + (z_r/f_P)^2}}\, w_0 \ , \tag{109}$$

where z_r and w_0 are the Rayleigh range and the beam waist of the incident beam, respectively, and f_P is the focal distance of the atomic lens.

5.2 Ramsey interferometry with focused atomic beam and Gouy phase

In order to experimentally observe this effect we propose an experiment with a focused Gaussian atomic beam. We will use a cylindrical focusing in the x direction, without changing the beam wavefunction in the y direction, what makes the total Gouy phase be $\pi/2$. By the analogy of the Schrödinger equation with the paraxial Helmholtz equation (Yariv, 1991; Snyder & Love, 1991; Berman, 1997; Marte & Stenholm, 1997; da Paz et al., 2007), we see that the cavities act on the $|g\rangle$ component of the atomic beam as cylindrical lenses with focal distance f_P. If we have $f_P = d/2$, where d is the distance between the cavities C_1 and C_2, the system will behave like the illustration in Figure 9. The cavity C_1 will transform the $|g\rangle$ component of the wavefunction in a converging beam with the waist on a distance $d/2$ (represented by solid lines). After its waist, the beam will diverge until the cavity C_2. The $|g\rangle$ component of the wavefunction on the position of cavity C_2 will have the same width and the opposite quadratic phase of the state $\psi'_{cm}(x)$ above, so the cavity C_2 will transform the divergent beam in a plane-wave beam again. The $|i\rangle$ component of the wavefunction, on the other hand, propagates as a plane-wave beam all the time (represented by dashed lines), as its interaction with the field of the cavities C_1 and C_2 is considered to be very small.

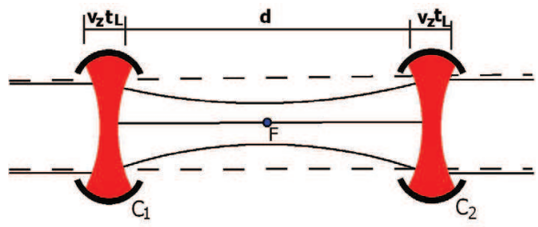

Fig. 9. Illustration of the operation of the cavities C_1 and C_2 as thin lenses for the atomic beam. The dashed lines represent the waist of the atomic beam if the cavities are empty. If a field is present, the solid lines represent the waist of a beam composed by atoms in the state $|g\rangle$. F denotes the focus region. On the other hand, if the beam is composed by atoms in the state $|i\rangle$, the waist does not change significatively.

By virtue of the $|g\rangle$ component acquires a $\pi/2$ Gouy phase due to the cylindrical focusing that is not shared by the $|i\rangle$ component, the interference pattern will be (da Paz et al., 2011)

$$P' = \cos^2[(\omega_r - \omega_{gi})t - \pi/2] \, . \tag{110}$$

The difference on the positions of the minimums and maximums of the patterns, one constructed when the field that forms the atomic lenses is present on the cavities C_1 and C_2 and other when the field is removed, should attest the existence of the Gouy phase for matter waves.

5.3 Experimental parameters and discussion

As experimental parameters, we propose the velocity of the atoms $v_z = 50$ m/s and a slit that generates an approximately Gaussian wavefunction for the atoms $\psi_0(x) \propto \mathrm{e}^{-x^2/w_0^2}$ with $w_0 = 10$ μm. The mass of Rubidium is $m = 1.44 \times 10^{-25}$ kg. With these parameters, the Rayleigh range of the atomic beam will be $z_r = k_P w_0^2/2 \simeq 3.5$ m, much larger than the length of the experimental apparatus, what justifies the plane-wave approximation. On the cavities C_1 and C_2, we consider an interaction time between the atoms and the atomic lenses $t_L = 0.2$ ms, that corresponds to a width $v_z t_L = 1$ cm for the field on the cavities. The

wavelength of the field of the cavities C_1 and C_2 must be $\lambda \simeq 5.8$ mm (Raimond et al., 2001), with frequency near but strongly detuned from the resonance of the transition $|g\rangle \Leftrightarrow |e\rangle$. The Rabi frequency is about $\Omega_0/(2\pi) = 47$ kHz (Raimond et al., 2001) and the detuning chosen is $\Delta_g/(2\pi) = -30$ MHz, what makes $\Delta_i/(2\pi) = +3.2$ GHz, such that with $\bar{n} = 3 \times 10^6$ photons, an effectively classical field, the focal distance for the atomic lenses is 10.5 cm for the $|g\rangle$ component and -11 m for the $|i\rangle$ component of the wavefunction. These parameters are consistent with a separation of $d = 21$ cm between C_1 and C_2. All the proposed parameters can be experimentally achieved (Raimond et al., 2001; Nogues et al., 1999; Gleyzes et al., 2007). Using the proposed parameters, we have $z_r' \simeq 3$ mm and $w_0' \simeq 0.3\ \mu m$. The fact that $d \gg z_r'$ justifies our consideration that the $|g\rangle$ component of the beam acquires a $\pi/2$ Gouy phase.
The interaction between the atomic beam and the field in the cavities C_1 and C_2 depends on the position x, according to Equation (103). If we do not want that photons be absorbed by the atoms, it is important that $\bar{n}\Omega_0^2 k^2 x^2/(\Delta_g^2) \ll 1$ for the entire beam (Scully & Zubairy, 1997). We have $\bar{n}\Omega_0^2 k^2 w_0^2/(\Delta_g^2) \simeq 8 \times 10^{-4}$ for the proposed parameters, where w_0 is the beam width, showing that the absorption of photons can be disregarded.
The phase difference between the electronic levels is given by

$$2\phi_i - \phi_g = \left(\Delta_{gi} - \frac{\Delta_g}{2} - \frac{\Omega_{min}^2}{4\Delta_g} \right) t_L, \tag{111}$$

where the last term is a dispersive phase that occurs because the intensity of the electric field is not exactly zero in the node $x = \pi/2$ for real cavities. In this case is important that the cavities C_1 and C_2 have a large quality factor Q. In fact, the ratio between the maximum and the minimum of intensity in a cavity should roughly be the quality factor Q. So the $|g\rangle$ component of the beam also acquires a phase $\bar{n}\Omega_0^2 t_L/(\Delta_g Q)$ on the passage in each cavity, and this phase will be added to the accumulated Gouy phase. If we want that this undesired phase be smaller than Gouy phase, we need $Q > 10^6$ for our proposed parameters. This can also be experimentally achieved (Raimond et al., 2001; Nogues et al., 1999; Gleyzes et al., 2007).

6. Conclusion

From the strict theoretical point of view we have used the formal analogy between matter and light waves to show that the well known Gouy phase in the context of classical optics, besides its geometrical character, reflects correlations of the same sort a free particle obeying a matter wave equation. Conversely we have seen that matter waves may also present the exact analogous to the Gouy phase of quantum optics and elaborated an experiment to measure it. We hope this work might encourage the groups with the appropriate facilities to realize the experiment and, who knows, find important applications for this matter phase. The verification of the Gouy phase in matter waves has the possibility to generate a great amount of development in atomic optics, in the same way as the electromagnetic counterpart Gouy phase had contributed to electromagnetic optics. For instance, it can be used to construct mode converters for atomic beams and trapped atoms, with potential applications in quantum information.

7. Acknowledgments

The authors thank Dr. P. L. Saldanha by fruitful discussions on experimental proposal to measure the Gouy phase. This work was in part supported by the Brazilian agencies CNPq, Capes and Fapemig.

8. References

Yariv, A. (1991). *Optical Electonics*, Saunders College Publishers, Philadelphia.

Snyder, A. W., and Love, J. D. (1991). *Waveguide Theory*, Chapman and Hall, London.

Berman, P. R. (1997). *Atom Interferometry*, Academic Press, San Diego.

Marte, M. A. M., and Stenholm, S. (1997). Paraxial light and atom optics: The optical Schrödinger equation and beyond, *Phys. Rev. A* 56, 2940.

Nairz, O., Arndt, M., and Zeilinger, A. (2002). Experimental verification of the Heisenberg uncertainty principle for fullerene molecules, *Phys. Rev. A* 65, 032109.

Saleh, B. E. A., and Teich, M. C. (1991). *Fundamentals of Photonics*, John Wiley et Sons, New York.

Gouy, C. R. (1890). *Acad. Sci. Paris* 110, 1251.

Gouy, C. R. (1891). Sur la propagation anomale des ondes, *Ann. Chim. Phip. Ser. 6* 24, 145.

Mair, A., Vaziri, A., Weihs, G., and Zeilinger, A. (2001). Entanglement of the orbital angular momentum states of photons, *Nature* 412, 313.

Allen, L., Beijersbergen, M. W., Spreeuw, R. J. C., and Woerdman, J. P. (1992). Orbital angular momentum of light and the transformation of Laguerre-Gaussian laser modes, *Phys. Rev. A* 45, 8185.

Beijersbergen, M. W., Allen, L., van der Veen, H. E. L. O., and Woerdman, J. P. (1993). Astigmatic laser mode converters and transfer of orbital angular momentum, *Opt. Comm.* 96, 123.

McMorran, B. J., Agrawal, A., Anderson, I. M., Herzing, A. A., Lezec, H. J., McClelland, J. J., and Unguris, J. (2011). Electron Vortex Beams with High Quanta of Orbital Angular Momentum, *Science* 331, 192.

Siegman, A. E. (1986). *Lasers*, University Science Books, Mill Valley.

Viale, A., Vicari, M., and Zanghì, N. (2003). Analysis of the loss of coherence in interferometry with macromolecules, *Phys. Rev. A* 68, 063610.

Jackson, J. D. (1999). *Classical Electrodynamics*, Jonh Wiley, New York.

Mandel, L., and Wolf, E. (1995). *Optical Coherence and Quantum Optics*, Cambridge, New York.

Gase, R. (1994). Methods of quantum mechanics applied to partially coherent light beams, *J. Opt. Soc. Am. A* 11, 2121.

Ballentine, L. E. (1998). *Quantum Mechanics*, World Scientific Publishing Co. Pte. Ltd, Singapore.

Scully, M. O., and Zubairy, M. S. (1997). *Quantum Optics*, Cambridge University Press, Cambridge.

Fano, U. (1957). Description of States in Quantum Mechanics by Density Matrix and Operator Techniques, *Rev. Mod. Phys.* 29, 74.

Stoler, D. (1981). Operator methods in physical optics, *J. Opt. Soc. Am.* 71, 334.

Simon, R., and Mukunda, N. (1993). Bargman Invariant and the Geometry of the Gouy Effect, *Phys. Rev. Lett.* 70, 880.

da Paz, I. G. (2006). *Matter Waves and Paraxial Propagation of Light*, Department of Physics, UFMG, MG, Brazil.

da Paz, I. G. (2011). *Gouy phase in matter waves: from pure and mixed Gaussian states*, Department of Physics, UFMG, MG, Brazil.

Souza, L. A. M., Nemes, M.C., Santos, M. F., and Peixoto de Faria, J. G. (2008). Quantifying the decay of quantum properties in single-mode states, *Opt. Comm.* 281, 4694.

Boyd, R. W. (1980). Intuitive explanation of the phase anomaly of focused light beams, *J. Opt. Soc. Am.* 70, 877.

Hariharan, P., and Robinson, P. A. (1996). The Gouy phase shift as a geometrical quantum effect, *J. Mod. Opt.* 43, 219.
Feng, S., Winful, H. G., and Hellwarth, R. W. (1998). Gouy shift and temporal reshaping of focused single-cycle electromagnetic pulses, *Opt. Lett.* 23, 385.
Feng, S., and Winful, H. G. (2001). Physical origin of the Gouy phase shift, *Opt. Lett.* 26, 485.
Yang, J., and Winful, H. G. (2006). Generakized eikonal treatment of the Gouy phase shift, *Opt. Lett.* 31, 104.
Holme, N. C. R., Daly, B. C., Myaing, M. T., and Norris, T. B. (2003). Gouy phase shift of single-cycle picosecond acoustic pulses, *Appl. Phys. Lett.* 83, 392.
Zhu, W., Agrawal, A., and Nahata, A. (2007). Direct measurement of the Gouy phase shift for surface plasmon-polaritons, *Opt. Express* 15, 9995.
Feurer, T., Stoyanov, N. S., Ward, D. W., and Nelson, K. A. (2002). Direct Visualization of the Gouy Phase by Focusing Phonon Polaritons, *Phys. Rev. Lett.* 88, 257.
Horvath, Z. L., and Bor, Z. (1999). Reshaping of femtosecond pulses by the Gouy phase shift, *Phys. Rev. E* 60, 2337.
Horvath, Z. L., Vinko, J., Bor, Z., and von der Linde, D. (1996). Acceleration of femtosecond pulses to superluminal velocities by Gouy phase shift, *Appl. Phys. B* 63, 481.
Gbur, G., Visser, T. D., and Wolf, E. (2002). Anomalous Behavior of Spectra near Phase singularities of Focused Waves, *Phys. Rev. Lett.* 88, 013901.
Nairz, O., Arndt, M., and Zeilinger, A. (2000). Experimental chanllenges in fullerene interferometry, *J. Modern Opt.* 47, 2811.
da Paz, I. G., Nemes, M. C., and Peixoto de Faria, J. G. (2007). Gouy phase and matter waves, *J. Phys.: Conference Series* 84, 012016.
da Paz, I. G., Monken, C. H., Padua, S., Nemes, M. C., and Peixoto de Faria, J. G. (2010). Indirect evidence for the Gouy phase for matter waves, *Phys. Lett. A* 374, 1660.
da Paz, I. G., Saldanha, P. L., Nemes, M. C., and Peixoto de Faria, J. G. (2011). Experimental proposal for measuring the Gouy phase for matter waves, *To be published* arXiv:1012.3910v1 [quant-ph].
Averbukh, I. S., Akulin V. M., and Schleich, W. P. (1994). Quantum Lens for Atomic Waves, *Phys. Rev. Lett.* 72, 437.
Rohwedder, B., and Orszag, M. (1996). Quantized light lenses for atoms: The perfect thick lens, *Phys. Rev. A* 54, 5076.
Schleich, W. P. (2001). *Quantum Optics in Phase Space*, Wiley-VCH, Berlin.
Bialynicki-Birula, I. (1998). Nonstandard Introduction to Squeezing of the Electromagnetic Field, *Acta Phys. Polonica B* 29, 3569.
Piza, A. F. R. T. (2001). *Mecânica Quântica*, Edusp, São Paulo.
Born, M., and Wolf, E. (1999). *Principles of Optics*, Cambridge University Press, Cambridge.
Ashkin, A. (1970). Acceleration and Trapping of Particles by Radiation Pressure, *Phys. Rev. Lett.* 24, 156.
Gordon, J. P., and Ashkin, A. (1980). Motion of atoms in a radiation trap, *Phys. Rev. A* 21, 1606.
Bjorkholm, J. E., Freeman, R. R., Ashkin, A., and Pearson, D. B. (1978). Observation of Focusing of Neutral Atoms by the Dipole Forces of Resonance-Radiation Pressure, *Phys. Rev. Lett.* 41, 1361.
Raimond, J. M., Brune, M., and Haroche, S. (2001). Colloquium: Manipulating quantum entanglement with atoms and photons in a cavity, *Rev. Mod. Phys.* 73, 565.

Nussenzveig, P., Bernardot, F., Brune, M., Hare, J., Raimond, J. M., Haroche, S., Gawlik, W. (1993). Preparation of high-principal-quantum-number “circular" states of rubidium, *Phys. Rev. A* 48, 3991.

Gallagher, T. F. (1994). *Rydberg Atoms*, Cambridge University Press, Cambridge.

Ramsey, N. F. (1985). *Molecular Beams*, Oxford University Press, New York.

Kim, J. I., Romero Fonseca, K. M., Horiguti, A. M., Davidovich, L., Nemes, M. C., and Toledo Piza, A. F. R. (1999). Classical behavior with small quantum numbers: the physics of Ramsey interferometry of Rydberg atoms, *Phys. Rev. Lett.* 82, 4737.

Gerry, C., and Knight, P. (2005). *Introductory Quantum Optics*, Cambridge University Press, Cambridge.

Nogues, G., Rauschenbeutel, A., Osnaghi, S., Brune, M., Raimond, J. M., and Haroche, S. (1999). Seeing a single photon without destroying it, *Nature* 400, 239.

Gleyzes, S., Kuhr, S., Guerlin, C., Bernu, J., Deleglise, S., Hoff, U. B., Brune, M., Raimond, J. M., and Haroche, S. (2007). Quantum jumps of light recording the birth and death of a photon in a cavity, *Nature* 446, 297.

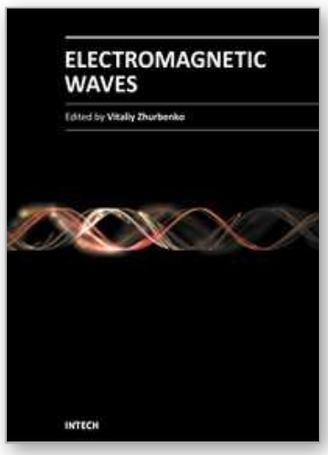

Electromagnetic Waves
Edited by Prof. Vitaliy Zhurbenko

ISBN 978-953-307-304-0
Hard cover, 510 pages
Publisher InTech
Published online 21, June, 2011
Published in print edition June, 2011

This book is dedicated to various aspects of electromagnetic wave theory and its applications in science and technology. The covered topics include the fundamental physics of electromagnetic waves, theory of electromagnetic wave propagation and scattering, methods of computational analysis, material characterization, electromagnetic properties of plasma, analysis and applications of periodic structures and waveguide components, and finally, the biological effects and medical applications of electromagnetic fields.

InTech Europe
University Campus STeP Ri
Slavka Krautzeka 83/A
51000 Rijeka, Croatia
Phone: +385 (51) 770 447
Fax: +385 (51) 686 166
www.intechopen.com

InTech China
Unit 405, Office Block, Hotel Equatorial Shanghai
No.65, Yan An Road (West), Shanghai, 200040, China
中国上海市延安西路65号上海国际贵都大饭店办公楼405单元
Phone: +86-21-62489820
Fax: +86-21-62489821

IntechOpen